Journal of Power Sources 247 (2014) 865–875

Contents lists available at ScienceDirect

Journal of Power Sources

journal homepage: www.elsevier.com/locate/jpowsour

A study of tetrabromobisphenol A (TBBA) as a flame retardant additive for Li-ion battery electrolytes

Dmitry G. Belov*, D.T. Shieh

Material and Chemical Research Laboratories, Industrial Technology Research Institute (ITRI), Hsinchu 31040, Taiwan

HIGHLIGHTS

- TBBA as a flame retardant additive in an electrolyte for Li-ion battery.
- Flammability mechanism of the battery/electrolyte: condensed-phase or gas-phase.
- TBBA undergo redox decomposition by oxidation reaction on the cathode surface.
- Even 1 wt.% of TBBA will sufficiently depress electrolyte flammability.

GRAPHICAL ABSTRACT

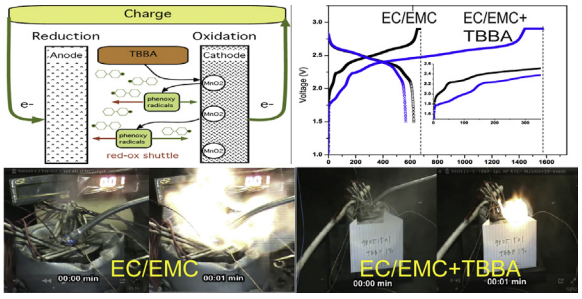

ARTICLE INFO

Article history:
Received 25 May 2013
Received in revised form
4 August 2013
Accepted 21 August 2013
Available online 18 September 2013

Keywords:
Flame retardant
Electrolyte flammability
Lithium-ion batteries
Tetrabromobisphenol A

ABSTRACT

Electrochemical behavior and flammability of tetrabromobisphenol A (TBBA)-mixed electrolyte solutions are investigated using 1 mol L^{-1} $LiPF_6$-EC:EMC (1:2 vol.%) with 0 wt.% (reference electrolyte) and 1–3 wt.% of TBBA. The cycling performance (at room and elevated temperature) and rate capability of the 18650 cell ($LiMn_2O_4$:$Li(Ni_{1/3}Co_{1/3}Mn_{1/3})O_2$ (8:2)/$Li_4Ti_5O_{12}$) cell containing TBBA-mixed electrolyte is similar to that of cell containing the reference electrolyte. A detailed analysis of the surface on both the anode and the cathode electrodes via X-ray photoelectron spectroscopy (XPS) indicated that the cathode electrode contains more Br components than the anode electrode. Within the first few cycles, on the positive electrode, we observe competing redox processes between the cathode material containing Mn and TBBA, which generate hydroxy radicals and other by-products. This process and the electrochemical reductive decomposition of TBBA to HBr, Br_2 and bisphenole A are responsible for the increased flame retardant properties of the electrolyte containing TBBA. Safety tests were performed using an 18650 cell showed that even 1 wt.% of TBBA in the electrolyte significantly reduces cell flammability.

1. Introduction

Li-ion batteries are used to power many electronic devices and increasingly motor vehicles, however, safety remains a major concern. The first attempts to improve battery safety focused on the incorporation of safety devices into the cell design. Small cylindrical lithium-ion cells (such as 18650) typically have a positive pin in the header. The header (crimp-sealed to the can body with a gasket to electrically isolate the negative can body from the positive header) contains: a positive temperature coefficient (PTC) device, a vent mechanism and a current interrupt device (CID). In prismatic lithium-ion cells where the header is welded to (and so in direct electrical contact with) the can body various devices can be placed outside battery, such as a negative temperature coefficient (NTC) thermistor, thermal fuse, etc. Soft-pack/pouch cells design (so-called “polymer batteries”) cannot employ many of the above-mentioned safety protection devices owing to their considerably different construction. Substantial variations in battery chemistry

* Corresponding author. Tel.: +886 3 5913129; fax: +886 3 5820039.
E-mail addresses: dmitri.white@gmail.com, dm.belov@live.com (D.G. Belov).

0378-7753/$ – see front matter © 2013 Elsevier B.V. All rights reserved.
http://dx.doi.org/10.1016/j.jpowsour.2013.08.143

and configuration mean that such protection devices are unable to effectively monitor cell behavior, health and safety level. It has been shown that overcharge and related soft shorting is the main source of Li-ion battery failure in battery packs. Since 2000 many attempts have been made to design chemical mechanisms that protect Li-ion batteries internally against overcharge through the implementation of various electrolyte additives [1–3]. Nevertheless, most of these attempts have failed due to the inability of chemical additives to create a reliable protective mechanism (such as an insulating or semi-conducting film) or initiate a shuttle mechanism under real conditions [4].

Another progressive approach to improve Li-ion battery safety is to utilize non-flammable electrolytes and flame retardant additives (such research increased significantly from 2005 onwards). Many kinds of nonflammable or flame-retardant electrolyte systems have been proposed [5–8]. These types of electrolytes include (a) phosphorous and fluorinated compounds known as flame-retardants that are used in many industries (such as polymer, textile, etc.), and (b) ionic liquids. Most of the flame retardant compounds added to electrolytes (1) undergoes reductive decomposition on graphite anodes [9], and (2) must exceed more than 15 %vol. or wt.% content in the electrolyte solution to be effective. Moreover, the high viscosity of most phosphorous flame-retardants and the relatively high cost fluorinated compounds can be prohibitive. Ionic liquids are also high-priced and only some meet the electrochemical [10] and safety [11] requirements for Li-ion batteries, mainly in combination with regular electrolytes [12,13].

The need to develop a safe and non-flammable electrolyte arises from the fact that all Li-ion batteries can catch fire under certain conditions. Not even the presence of external protection devices can guarantee their safety. In most safety tests the main trigger of exothermic reactions leading to the catastrophic failure of Li-ion batteries involving explosions and/or fire is the highly reactive and flammable liquid electrolytes that are currently and widely used.

Among the wide range and variety of flame-retardants available, there is one class that has rarely been studied as an electrolyte additive in Li-ion batteries, that is, the brominated compounds. In our study, we tested tetrabromobisphenol A (TBBA) as a flame-retardant additive for Li-ion battery electrolytes. TBBA is widely used in many industries as flame-retardant. In general, brominated flame-retardants are divided into two categories, “additive” and “reactive”, according to the mechanism of termination of flame propagation: TBBA belongs to the latter category.

Here, we present our study on the efficiency of TBBA as a flame-retardant additive in a common non-aqueous electrolyte for use in Li-ion batteries. The influence of TBBA additive amount (from 0 to 3 wt.% in the electrolyte) on the electrolyte and over-all battery properties at different current rates and temperatures is evaluated. A detailed analysis of the surface on both the anode and the cathode electrodes is conducted via X-ray photoelectron spectroscopy (XPS). Flammability testing of the electrolyte is performed using a full cell (18650-type).

2. Experimental

2.1. Electrolyte

1 M $LiPF_6$, EC:EMC (1:2 vol.), VC (2 wt.%) (denoted as E1) was purchased from Ferro (moisture less than 20 ppm) for use as a reference electrolyte and base for mixing with TBBA. 3,3′,5,5′-tetrabromobisphenol A (TBBA) was purchased from Aldrich and stored in a glove box prior to use. TBBA is a colorless solid (Table 1) insoluble in H_2O, with chemical structure as shown in Fig. 1. Electrolyte solutions were prepared in a “dry room” atmosphere by mixing E1 with 1, 2 and 3 wt.% of TBBA for 1 h (denoted as E2, E3, E4, respectively). Molar concentrations are 0.018, 0.036 and 0.055 M, respectively. Final electrolyte solutions were colorless and showed no change in conductivity at room temperature when compared to the reference electrolyte (9.1 mS cm^{-1}) (tested by conductivity meter: WTW/Cond 330i/SET (Germany) conductivity meter with GC electrodes) and moisture.

Table 1
Properties of some organic electrolyte solvents and TBBA.

	T_b/°C	T_f/°C	T_m/°C	d/g cm^{-3} (20 °C)
EC	248	160	36.4	1.32
PC	240	132	−55	1.21
EMC	110	22.5	−53	1.01
DMC	91	18	4.6	1.07
DEC	126	31	−74.3	0.97
TBBA	250		180	2.12

T_b – boiling temperature; T_f – flash temperature; T_m – melting temperature.

2.2. Coin-cell assembly

The positive electrode was fabricated using carbon-coated C–$LiFe_{1-y}Mn_yPO_4$, polyvinylidene difluoride (PVDF, Kureha) as the binder and Super-P carbon black as a conductive agent. The negative electrode consisted of graphite (MCMB 1028), PVDF and Super-P. The slurry of favorable positive and negative electrodes in *N*-methylpyrrolidinone (NMP) was then coated on a thin foil (aluminum and copper of 20 and 14 μm thickness, respectively) and dried for 12 h at 150 °C in a vacuum oven. Polyethylene separator was used in the electrochemical cells (2032-type coin-cells) and assembled in a “dry room” (dew point is −50 °C).

2.3. 18650 cell assembly

The positive electrode for 18650 cells was fabricated using a mix of $LiMn_2O_4$ and $Li(Ni_{1/3}Co_{1/3}Mn_{1/3})O_2$ as the active material in the ratio of 8:2, PVDF (Kureha) as the binder and a mix of Super-P and KS6 graphite as the conductive agents. The negative electrode $Li_4Ti_5O_{12}$ was fabricated using a PVDF (Kureha) binder and mix of Super-P and KS6. The design capacity of 18650 cells is 600 mAh at C/5.

2.4. Tests

The electrochemical stability of the electrolytes containing TBBA was measured by cyclic voltammetry (CV) of the coin cell. The potential was scanned between 0 and 1.2 V (for MCMB/Li) and 3 and 4.4 V (C–$LiFe_{1-y}Mn_yPO_4$/Li) versus Li/Li^+ at a scan rate of 0.1 mV s^{-1} with the Solartron SI1287 (Electrochemical Interface).

Charge–discharge (cycle life) tests were performed on $Li_4Ti_5O_{12}$/($LiMn_2O_4$:$Li(Ni_{1/3}Co_{1/3}Mn_{1/3})O_2$) 18650 cells at a charge–discharge rate of 1 C in the voltage range of 2.9–1.5 V for 100 cycles at 55 °C and room temperature. The rate capability of the cells was

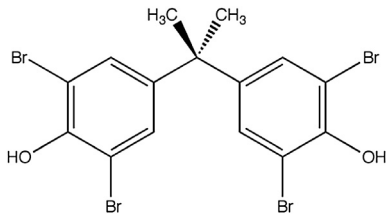

Fig. 1. TBBA structure.

evaluated via a constant current (CC) discharge at the following current drains: 1C, 2C, 3C, 5C, 8C and 10C. The tests were conducted using a multi-step constant-current/constant-voltage (CC/CV) technique charged to 2.9 V. Rate characteristics and cycle ability tests were investigated using a Bitrode battery cycler.

Morphology of the separator, positive and negative electrode surfaces was examined by scanning electron microscopy (SEM) (Hitachi S-3500H and S-4800) before and after 100 cycles. Prior to SEM investigation, samples were cautiously washed with DMC solvent in the "dry room" and dried in a vacuum.

Safety tests were carried out using an in-house fixture designed for 18650 cells, schematically presented on Fig. 2 and similar to [14]. The heating rate of the cell was 5 °C min^{-1}. SOC of the sample 18650 cells was 100%.

XPS analyses were carried out with a Kratos Axis Ultra spectrometer using a focused monochromatized Al Ka radiation ($h\nu$ = 1486.6 eV). The spectrometer was calibrated using the photoemission line Ag $3d_{5/2}$ binding energy (BE) 368.3 eV. For the Ag $3d_{5/2}$ line, the full width at half maximum (FWHM) was 0.61 eV under the recording conditions. Core peaks were recorded with 20 eV constant pass energy. An analyzed area of 300 um × 500 um was selected on samples, and the pressure in the analysis chamber set to ca. 5×10^{-7} Pa. After cycle tests cells were disassembled in a "dry room" atmosphere, and the washed electrodes were carefully mounted on a XPS stage. The binding energy of each spectrum for electrodes was calibrated by C 1s peak, corresponding to hydrocarbon adsorbed on the sample surface (285.0 eV). Core peaks were analyzed using a nonlinear Shirley-type background. The peak positions and areas were optimized by a weighted least-squares fitting method using 70% Gaussian, 30% Lorentzian line shapes. Quantification was performed according to Scofield's relative sensitivity factors [15].

3. Results and discussion

The TBBA molecule has several potential active centers in its structure: Br, OH and a center C atom (C–$(CH_3)_2$) located between rings. Although this molecule is relatively thermally stable (T_m > 180 °C, >250 °C decomposition), it is quite chemically and/or electrochemically reactive. To evaluate possible reduction/oxidation of the electrolyte containing TBBA a 2032-coin cell structure was used to test MCMB/Li and C–$LiFe_{1-y}Mn_yPO_4$/Li half-cells containing electrolytes: E1 and E4. Results are shown in Figs. 3 and 4.

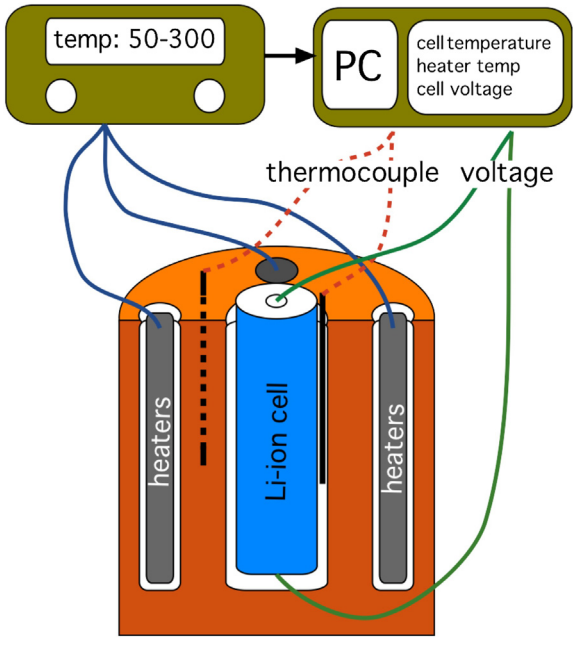

Fig. 2. Schematic drawing of the electrolyte safety test fixture.

3.1. Electrochemical investigations

CV data for the first three cycles of the MCMB/Li half-cells operating between 0 and 1.2 V with electrolytes E1 (0 wt.% TBBA) and E4 (3 wt.% TBBA) are shown in Fig. 3(a, b). During reductive (charge) or oxidative (discharge) scans of the MCMB electrode in the E4 electrolyte, no additional reactions were observed. The first scan shows a low intensity cathodic peak at ~0.2 V, which corresponds to the three order lithiation plateau and grows on subsequent scans. This is usually attributed to common side reactions that occur at the graphite surface (SEI_{anode}). The first scan of the cell containing E4 shows a slightly higher intensity for both oxidative and reductive peaks over the sample containing reference electrolyte E1. However, the second and third scans show that both oxidative and reductive peak intensity of the cell containing E4 were moderately lower than the cell containing E1. The scan rate

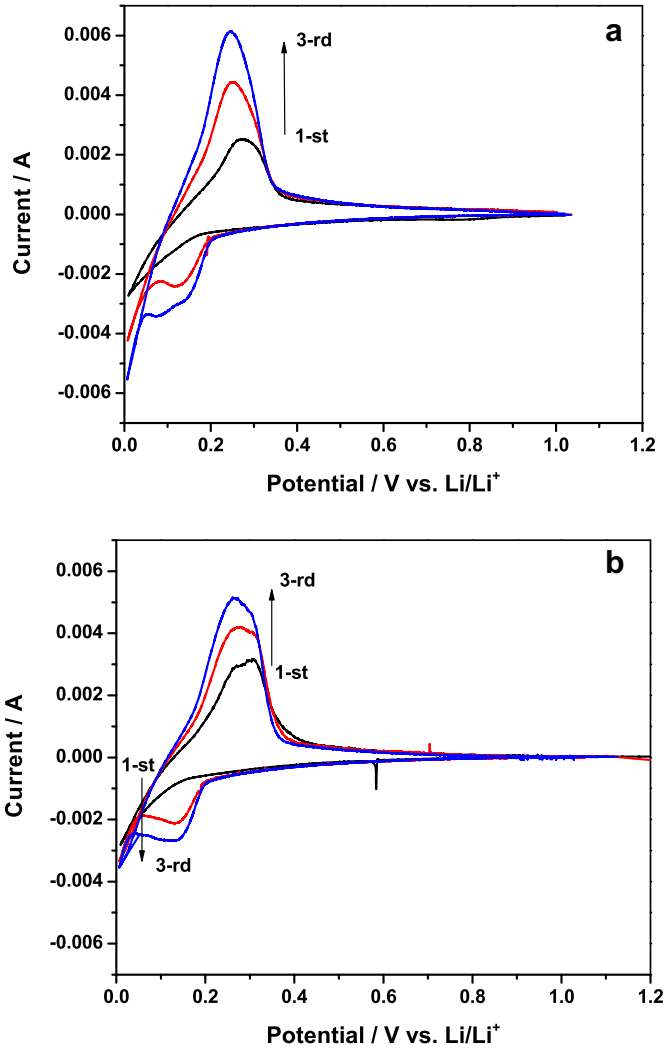

Fig. 3. CV curves for the first 3 cycles of the anodes in cells (MCMB vs. Li/Li^+) containing electrolyte: (a) E1 (0 wt.% TBBA), (b) E4 (3 wt.% TBBA). The potential was scanned from 1.2 V to 0 V at a 0.1 mV s^{-1} rate.

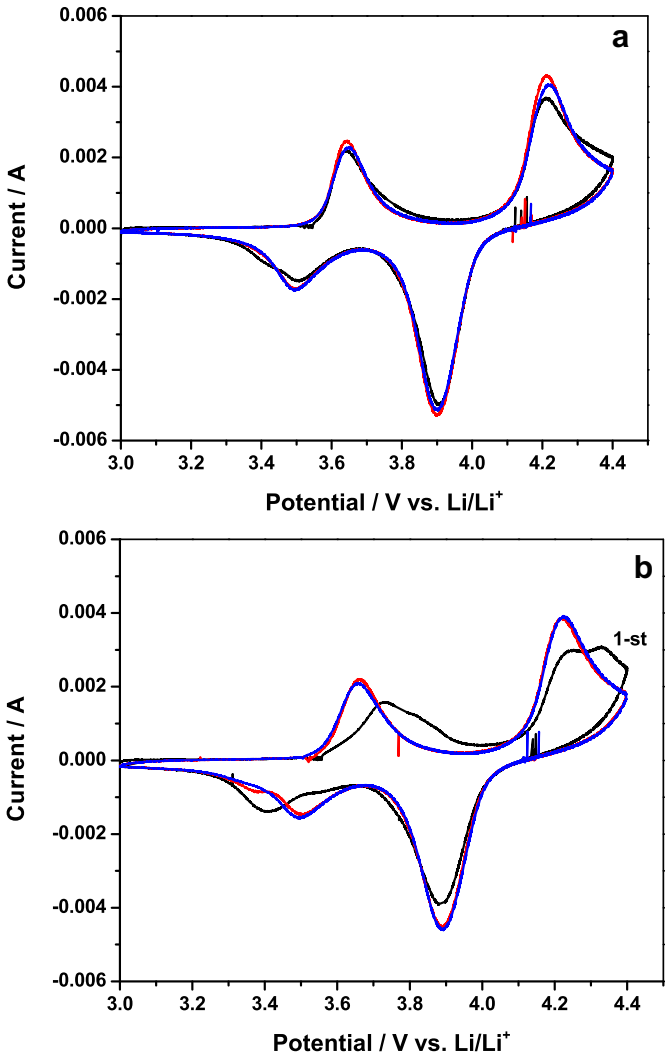

Fig. 4. CV of the C–$LiFe_{1-y}Mn_yPO_4$ vs. Li/Li^+ for the first 3 cycles with electrolyte: (a) E1 (0 wt.% TBBA), (b) E4 (3 wt.% TBBA). The potential was scanned from 3 V to 4.4 V at a 0.1 mV s^{-1} rate.

used in the CV test, 0.1 mV s^{-1}, was too fast to determine the real capacity of the Li-ion battery and less sensitive to the kinetic behavior of the electrode. We believe that the lower intensity of the CV peaks observed in the E4 electrolyte is a result of the slightly higher resistance of the SEI layer on the MCMB electrode generated in the presence of TBBA, as compared to the SEI generated in the presence of the reference electrolyte.

Fig. 4 shows the first three consecutive cycles measured with fresh cathode electrodes (C–$LiFe_{1-y}Mn_yPO_4$/Li) in electrolytes E1 and E4. In Fig. 4a, the cathode electrode in the presence of the reference electrolyte (E1) clearly shows reversible behavior with two oxidation peaks at ca. 3.6 and 4.2 V, the same characteristics as observed for Fe and Mn redox couples, respectively [16]. In Fig. 4b, the first cycle shows that the oxidative current of the two peaks is slightly smaller than that of subsequent cycles in the electrolyte containing TBBA. This indicates some oxidation reactions involving TBBA have occurred at the cathode surface, resulting in a higher over potential (deformed peak) and lower oxidation current in the initial cycle. However, the redox reactions involving C–$LiFe_{1-y}Mn_yPO_4$ revert to the normal in subsequent cycles, which indicates that TBBA is probably oxidized at ca. 3.5 V and forms a SEI layer ($SEI_{cathode}$) on the cathode that will slightly retards Li-ion intercalation.

All the data above indicates that no visible extra-peaks were created by TBBA on the anode or cathode electrodes. However, the presence of TBBA does slightly reduce cell capacity by forming a new structure of passivation layers (SEI). Slight depression/shifting of the initial oxidation/reduction peaks (from 3.65 V to 3.7 V and from 3.5 V to 3.4 V, respectively) on the cathode were noted. This was observed only during the first charge/discharge cycle. Such behavior is quite different that of to most types of flame retardants studied so far [17,18], where the majority of electrode degradation and electrolyte decomposition phenomena have been observed on the negative (graphite) electrode. Accordingly, on the basis of the conclusions and test results detailed above, we can exclude the side reactions of graphite with electrolyte/TBBA and focus attention on the study of positive electrode interaction involving TBBA.

3.2. Full cell performance (18650)

18650 cells, using $Li_4Ti_5O_{12}$ for the negative electrode and mixed cathodes ($LiMn_2O_4$:$Li(Ni_{1/3}Co_{1/3}Mn_{1/3})O_2$ = 8:2) for the positive electrode and E1, E2, E3 and E4 electrolytes, were assembled and tested. In contrast to graphite anodes that currently dominate the Li-ion battery market, $Li_4Ti_5O_{12}$ anodes have no SEI formation stage owing to a higher redox potential (1.55 V vs. Li/Li^+), making application of a very slow charge (such as C/20 or C/10) at the formation stage unnecessary. A cell activation process was nevertheless applied to the samples following their assembly, i.e., a relatively fast charge at C/5 (1C = 600 mAh) with constant-current (CC) up to 2.9 V followed by a constant-voltage (CV) charge with two regimes: (a) no time limit and (b) time limited charge (CC–CV): 10 h and rest 20 min; CC discharge at C/5 down to 1.5 V and rest on 20 min.

The results of the first charge/discharge cycles of the 18650 cells containing E1 and E4 electrolytes are reported in Fig. 5. They show a significant difference in capacity consumption for two identical (estimated capacity) samples at the first charge. Cells containing E1 electrolyte shows regular charge/discharge curves, however, samples containing E4 electrolyte show an almost triple charge capacity increase over the reference cell (E1). As shown in the inset on Fig. 5, the voltage curve started to plateau at around 1.8 V at C/5 rate, which suggests that some surface reaction occurred before Li intercalation/deintercalation into/from active materials in the E4

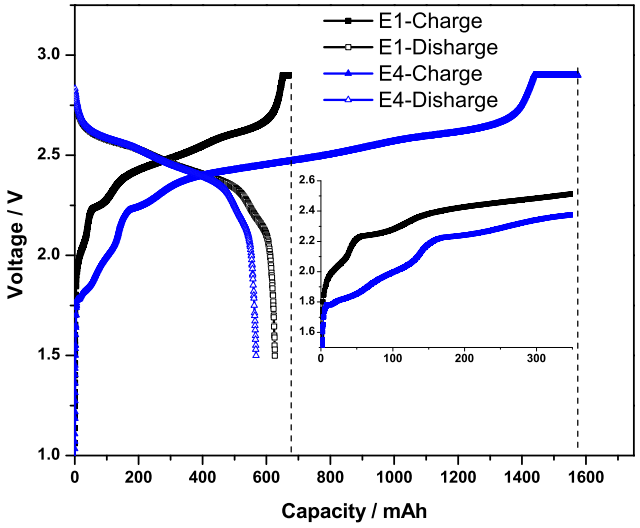

Fig. 5. First cycle of the 18650 cells ($Li_4Ti_5O_{12}$/$LiMn_2O_4$:$Li(Ni_{1/3}Co_{1/3}Mn_{1/3})O_2$) containing reference electrolyte E1 (0 wt.% TBBP) and E4 (3 wt.% TBBA) at C/5, voltages range 1.5–2.9 V, cut-off: 0.025C (C/40).

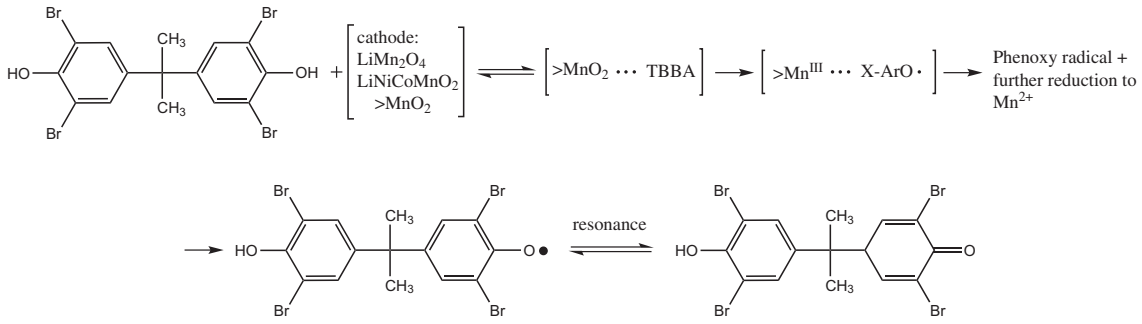

Fig. 6. First stage of oxidation reaction of the TBBA on the cathode surface by MnO_2 catalyst.

electrolyte. Due to the higher intercalation/deintercalation voltage of the $Li_4Ti_5O_{12}$ anode in the cell, the consumable charge can be assigned to the redox reactions of TBBA on the cathode surface.

We propose a two-phase mechanism for TBBA decomposition. The first phase is redox decomposition, which occurs on the cathode surface with subsequent oxidation of TBBA as schematically presented on Figs. 6 and 7. According to the oxidation path of TBBA on a mixed cathode surface with MnO_2 catalytic centers proposed by Lin at al. [19], TBBA is oxidized to form a phenoxy radical on the metal oxide surface and reducing the metal oxide (Mn^{IV} to Mn^{III}). The formed phenoxy radical may process further oxidation on the cathode surface and acts as a redox shuttle molecule [20,21], which is reduced on the anode surface after it diffuses back. The electrode surface reactions of TBBA consume the extra charge capacity in addition to the normal charge capacity during the first charge process. If TBBA acts as a redox shuttle agent on the fresh metal oxide surface, the charge capacity should be affected by the concentration of TBBA and the charge rate. The more TBBA added to the electrolyte, the higher the initial charge capacity obtained (so-call current leakage phenomena). Moreover, the higher the charge/discharge rate adopted, the higher the charge/discharge capacity obtained as less time is required for TBBA/phenoxy radicals to diffuse to the counter electrode. However, the live time for such radicals is relatively short, which explains the regular cycle behavior and reasonable rate performance of the battery with TBBA in the electrolyte (discussed later in this Section).

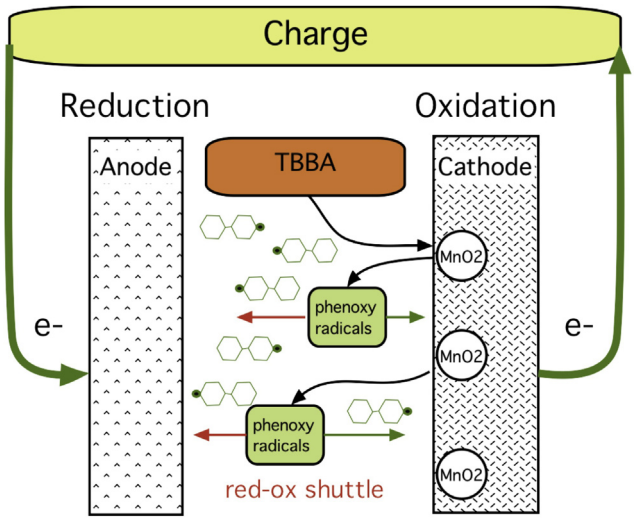

Fig. 7. Mechanism and representation of oxidation reaction of TBBA in the battery (first phase).

The second phase of TBBA decomposition occurs on heating of the battery and is followed by its reductive dehalogenation. In this phase, the main products of the remaining TBBA and by-products of its previous redox decomposition will be bisphenol A (BPA), HBr and Br_2 (discussion in Section 3.4).

The first phase of TBBA redox decomposition may be illustrated by the following experiments conducted at different rates of charge/discharge. In our tests we used C/2 and 1C current rate during the first charge/discharge cycle (formation) to understand the kinetics of competing reactions between Li^+ and TBBA on the electrode surface vs. TBBA concentration. The results of the first three charge/discharge cycles of the cells filled with four electrolytes (E1–E4) performed at C/2 rates (C = 600 mAh) are given on Fig. 8a–d.

The charge process used in this test employed a different (1) current rate (C/2 vs. C/5) and (2) time limit for charge step, i.e. the regime (b) (CC–CV limited to 10 h) from the test in Fig. 5. Consequently, a small deviation in discharge capacity was observed on Figs. 5 and 8a for the reference cell tested by C/5 and C/2 current (i.e. ~600 and ~550 mAh, respectively). The cell containing E2 electrolyte (Fig. 8b) shows an increase in first charge capacity up to ~165% vs. the reference cell, however, discharge capacity remains almost the same (530 mAh vs. 545 mAh).

Much larger differences are found when TBBA concentration is increased to 2 wt.% (E3) and 3 wt.% (E4) (Fig. 8c, d). For both samples, the first charge does not reach the CV part, due to the time limit (cut-off) of the charge program. Output (discharge) capacity decreases as the amount of TBBA in the electrolyte is increased and is subsequently proportional to the final charge voltage. The first charge in Fig. 8c is cut-off at 2.58 V, giving a first discharge capacity of 240 mAh. The first charge in Fig. 8d is cut-off at 2.39 V, giving a first discharge capacity of only 58 mAh and the third charge is cut-off at 2.55 V, giving a discharge capacity of 210 mAh. As pointed out above, electrons are drawn to the TBBA molecules first blocking or slowing down Li^+ intercalation/deintercalation into the anode and removing Li^+ from the cathode by current consumption. This reaction is rate and concentration dependent as seen in Figs. 8b–d and 9. In Fig. 9, two samples with the same amount of TBBA (E3) are charged at different current rates, C/5 and 1C and a time cut-off of 10 h applied for the CV part. The high-current rate (1C) allows Li^+ to be intercalated at close to theoretical capacity at discharge while the low current rate (C/5) process significantly suppresses Li^+ intercalation, with only 20 mAh capacity at discharge.

To evaluate the performance of Li-ion cells containing TBBA additive in the electrolyte, we performed the cycle tests on the 18650 cells at room temperature and in elevated temperature conditions (55 °C) at 1C current rate. Fig. 10 shows the cycle profiles of four types of electrolyte (E1–E4) at room temperature. As expected, the initial discharge capacity for the electrolyte with the highest TBBA concentration (E4) is the lowest: E4 < E3 < E2 = E1.

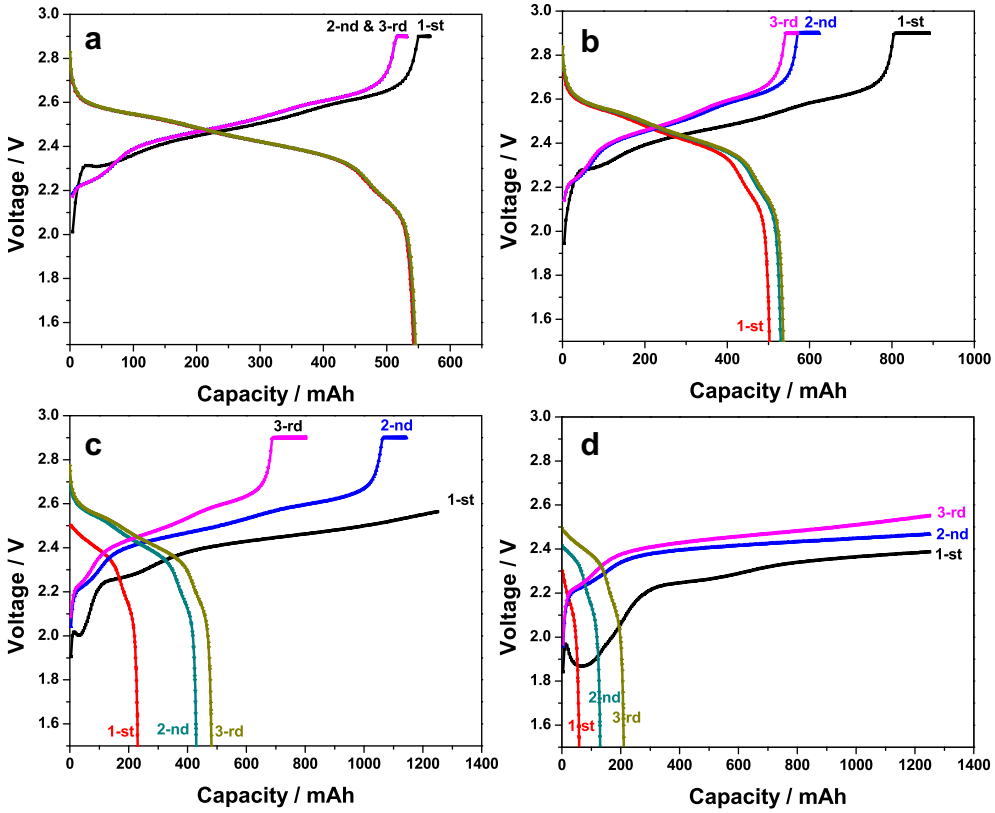

Fig. 8. First three charge–discharge cycles of 18650 cells ($Li_4Ti_5O_{12}/LiMn_2O_4$:$Li(Ni_{1/3}Co_{1/3}Mn_{1/3})O_2$) filled with control electrolyte: (a) E1 (0 wt.% TBBA), (b) E2 (1 wt.% TBBA), (c) E3 (2 wt.% TBBA), (d) E4 (3 wt.% TBBA) at C/2 rate, voltage range 1.5–2.9 V, cut-off time: 5 h at CV period.

However, on about the 10-th cycle all cells reaches nearly equal capacities. No obvious capacity fading related to TBBA presence was found after almost 100 cycles. Fig. 11 shows high-temperature cycle profiles for the same electrolytes are presented as capacity retention (%). The initial 10 cycles were substituted (normalized) to an equal value. No differences in samples performance after 100 cycles were observed.

After room and high-temperature cycle tests (100 cycles) two samples (E1 and E3) were dismantled, electrodes and separator were recovered from the cells in an argon glove box and examined by SEM. On the electrode surface (both anode and cathode) and separator cycled at room temperature no differences were found for samples cycled with either reference electrolyte E1 or with electrolyte E3 (not shown here). Only on the separator surface of the sample E3 cycled at the high temperature, was a small amount

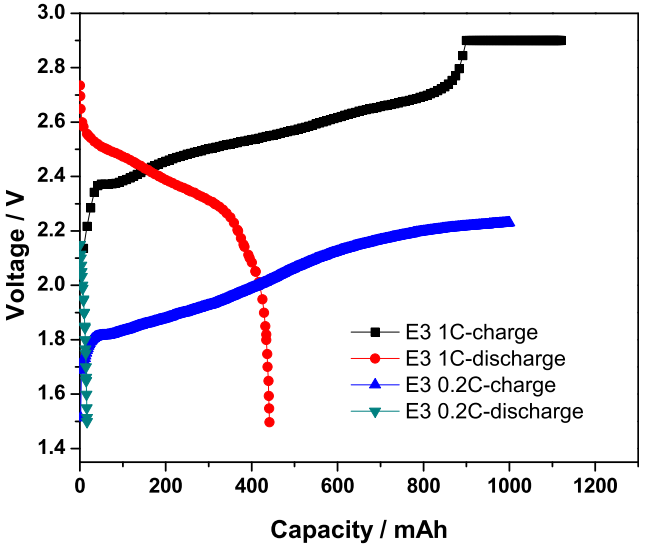

Fig. 9. First charge–discharge cycles of 18650 cells ($Li_4Ti_5O_{12}/LiMn_2O_4$:$Li(Ni_{1/3}Co_{1/3}Mn_{1/3})O_2$) filled with electrolyte E3 (2 wt.% TBBA) at C/5 and 1C current rate with charge time limit at 10 h and 3 h, respectively.

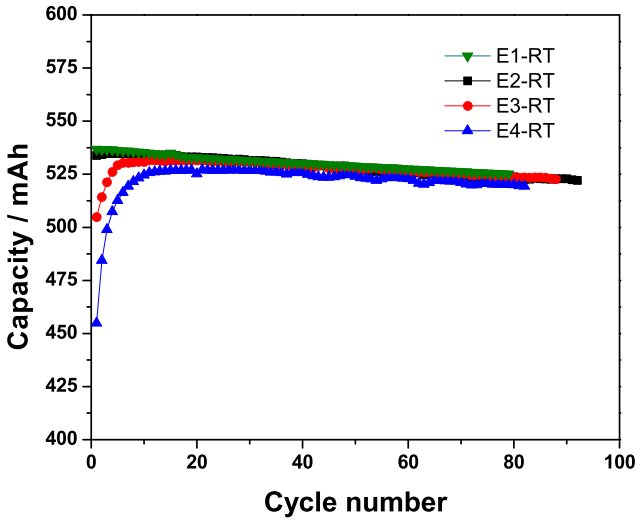

Fig. 10. Cycle performance of the 18650 ($Li_4Ti_5O_{12}/LiMn_2O_4$:$Li(Ni_{1/3}Co_{1/3}Mn_{1/3})O_2$) cells with 0–3 wt.% of TBBA in electrolyte (E1–E4) at 1C/1C charge/discharge (room temperature).

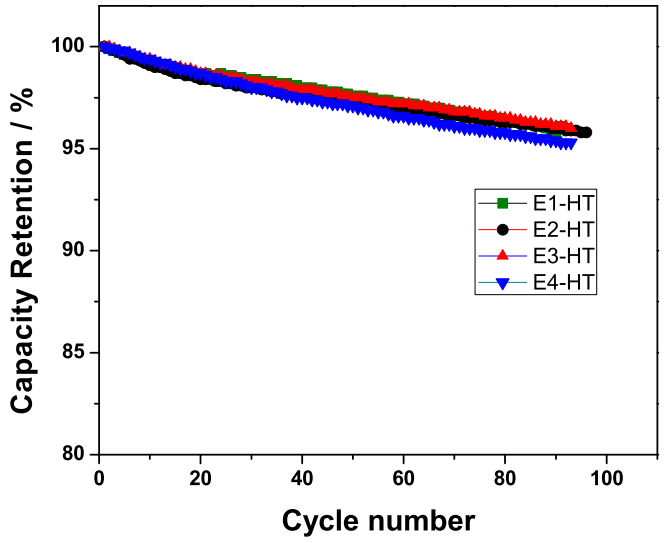

Fig. 11. Cycle performance of the 18650 ($Li_4Ti_5O_{12}$/$LiMn_2O_4$:$Li(Ni_{1/3}Co_{1/3}Mn_{1/3})O_2$) cells with 0–3 wt.% of TBBA in electrolyte (E1–E4) at 1C/1C charge/discharge (high temperature: 55 °C).

of by-product precipitation found (Fig. 12). As seen in Fig. 12b, spherical bleached spots formed on the separator surface during the high temperature cycle. The nature of these white spots is more than likely bisphenol A and requires more precise investigations. However, according to our tests and the discussion above, the presence of TBBA in the electrolyte had very little influence on cell performance. The amount of by-products precipitated at the separator surface is negligible as seen in Fig. 12c and only appear after prolonged cycling at a high temperature.

Fig. 13 shows the high rate discharge test of 18650 cells containing various electrolytes. The presence of TBBA in the electrolyte does not influence cell performance up to a 5C discharge rate, nor does it significantly decrease cell performance at higher rates (<5% of capacity retention).

3.3. XPS analysis of the anode and cathode surface film

After 100 cycles in 18650 cells with E1 and E4 electrolytes at 55 °C the following elements were detected on the surface of both electrodes: C, F, O, Mn, Br. The atomic composition (%) of electrode surfaces is presented in Table 2.

Fig. 14 shows high-resolution XPS spectra for Br 3d5/2 regions of surface films on the anode (Fig. 14A) and cathode (Fig. 14B) in cells cycled with electrolytes E1 (a) and E4 (b) (and sputter cleaned for 5 s), and E4 after 5 min etching (c). XPS spectra of the anode and cathode surfaces cycled with E1 electrolyte after 5 min etching showed no change and are not shown here. In contrast, both electrodes cycled with E4 electrolyte show peaks at 70.4 eV corresponding to Br (assigned to bromophenol) with a shoulder at 68.7 eV (assigned to LiBr) that were still detectable after 5 s of etching (Fig. 14A/B-b). However, the Br 3d5/2 core peak of the anode electrode almost disappeared after 5 min etching (Fig. 14A-c anode). On the cathode, the peak at 70.4 eV remained even after 5 min etching (Fig. 14B-c cathode). Such different Br distribution on the anode and cathode electrode surfaces is in agreement with tests and assumptions described above, i.e., that TBBA's redox reaction takes place mainly on the cathode electrode. Although some Br compounds can be detected on both the surfaces of the cathode and anode, the Br compounds are easily removed from the anode but a significant amount still remains on the cathode even after 5 min sputter etching. When TBBA is reacted with the cathode, it forms a complex, thick and stable solid-state passivation layer. The small Br signal that was detected on the fresh anode surface is mainly due to

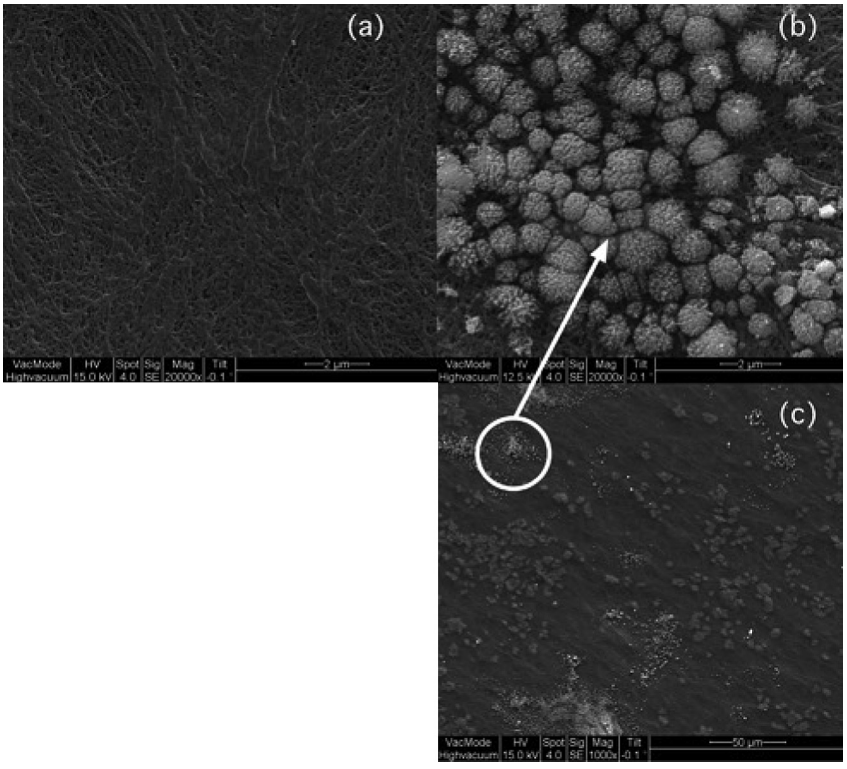

Fig. 12. SEM picture of the separator surface after high temperature cycling: (a) sample with control electrolyte E1, (b) sample with E3 (2 wt.% TBBA), (c) low resolution of (b).

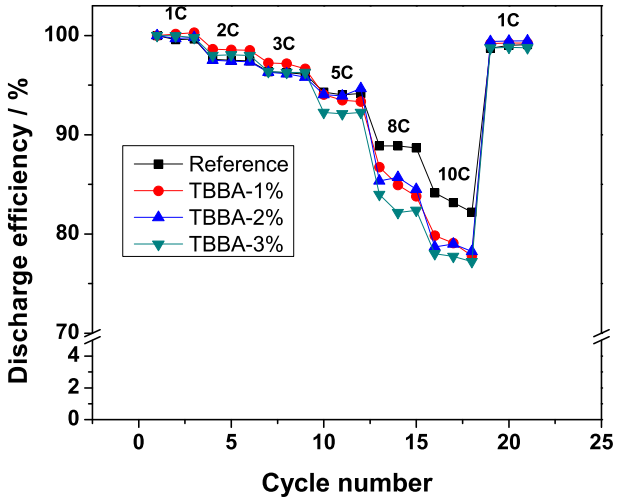

Fig. 13. Rate performance of the 18650 ($Li_4Ti_5O_{12}$/$LiMn_2O_4$:$Li(Ni_{1/3}Co_{1/3}Mn_{1/3})O_2$) cells with E1, E2, E3 and E4 electrolytes (0–3 wt.% of TBBA).

the precipitation of TBBA and/or its by-products from reactions on the cathode, which may be easily cleaned off by etching.

3.4. Safety testing and mechanism of flame retarding

This application of TBBA as a flame-retardant additive in Li-ion battery electrolytes was motivated by general concerns about battery flammability and specific interest in the mechanism of flame retarding in Li-ion battery/electrolyte in particular.

Most common flame-retardants may be divided into two categories according to their mechanism of flame retarding: condensed-phase and gas-phase. Fire extinguishing mechanisms for Li-ion batteries may take one of two forms or both: (1) inside the battery (to reduce the amount of flammable fuel and heat generated), and (2) outside the battery (to extinguish gaseous flammable products when the battery vents or even explodes). The first mechanism occurs in the condensed phase, i.e., inside the battery body, in several stages. This is the most complicated case as it may be caused by either self-heating, i.e., an internal source of heat (overcharge, micro-shorting, high charge/discharge rate) or external heat. The second mechanism occurs in the in gas-phase. These two cases display significant differences and require different types of flame-retardants.

To evaluate the mechanism and efficiency of TBBA additive as a flame retardant in the electrolyte, we tested several 18650 cells in the safety test fixture described in Section 2.4. After setting up the testing cell into the fixture, its temperature was raised slowly at the rate of 5 °C min^{-1} up to 200 °C. When the pressure inside the cell

Table 2
Element surface concentrations (atom%).

	C 1s	O 1s	F 1s	Mn 2p	Br 3d
Anode					
E1 (TBBP 0%), 5 s cleaning	54.8	19.9	17.92	0.55	0.01
E1 (TBBP 0%), 5 min etching	46.49	26.9	12.11	0.01	0.00
E4 (TBBP 3%), 5 s cleaning	50.95	20.1	23.51	1.36	0.47
E4 (TBBP 3%), 5 min etching	42.46	27.6	16.21	0.25	0.01
Cathode					
E1 (TBBP 0%), 5 s cleaning	66.01	11.8	19.18	2.96	0.03
E1 (TBBP 0%), 5 min etching	65.14	12.6	10.97	11.25	0.02
E4 (TBBP 3%), 5 s cleaning	57.15	14.2	25.19	1.37	2.01
E4 (TBBP 3%), 5 min etching	55.73	12.8	19.93	10.25	1.26

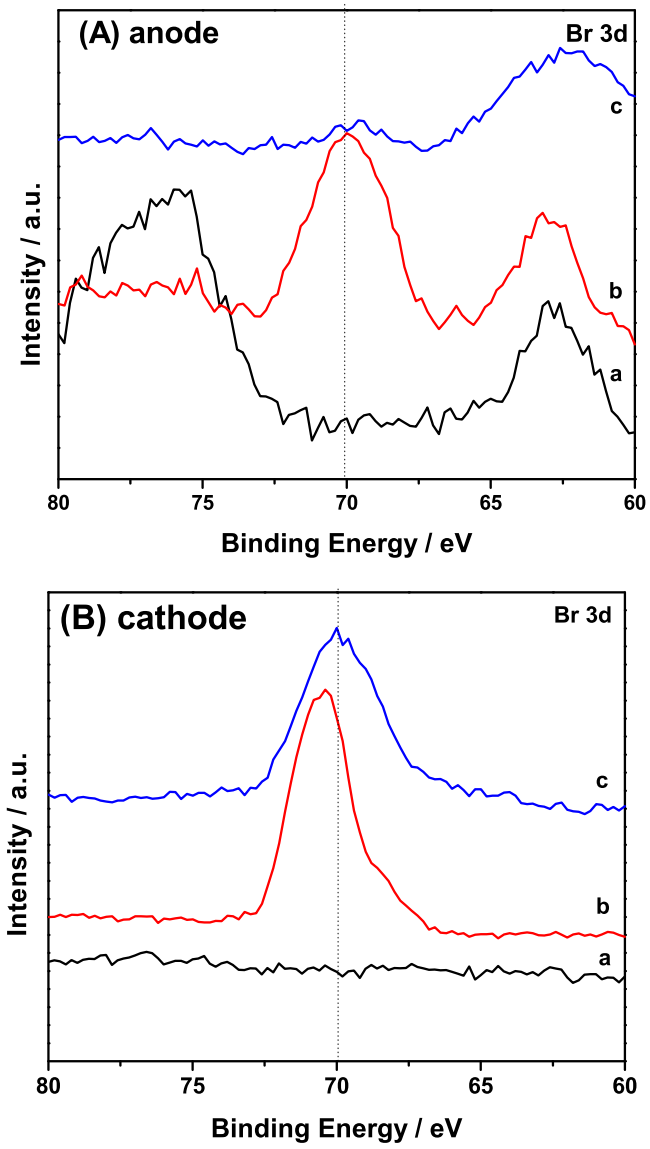

Fig. 14. XPS spectra (Br 3d5/2) of the surface film on the (A) $Li_4Ti_5O_{12}$ anode and (B) $LiMn_2O_4$:$Li(Ni_{1/3}Co_{1/3}Mn_{1/3})O_2$ cathode electrode (after 100 cycles of the cells with E1 and E4 electrolytes) at 55 °C. (a) – (E1) surface; (b) – (E4) surface; (c) – (E4) surface after 5 min etching.

reached the limit of the safety valve device, the pressure vent opened (or the gasket melted), releasing a gaseous and liquid mixture of electrolyte and its by-products. This occurred when the cell's skin reached a temperature of 140 °C and above, at which point, the igniter on the top of the cell started to produce sparks inside the electrolyte steam flow.

Several 18650 cells containing reference electrolyte (E1) and electrolytes with TBBA (E2, E3, E4) were tested. All samples were cycled for 100 cycles at room and high temperatures before undergoing the flammability test. The criteria used in the flammability test were ignition and duration of flaming.

The electrolyte steam from the reference cell ignited immediately upon venting and burned intensely. The flame burned continuously for 12 min until all the liquid electrolyte and concomitant gaseous products had exited the cell (Fig. 15). Cells filled with E2 electrolyte (1 wt.% TBBA) were also tested after 100 cycles at a room and high temperatures. A low profile fire was obtained on release of gaseous and liquid mixtures of electrolyte E2

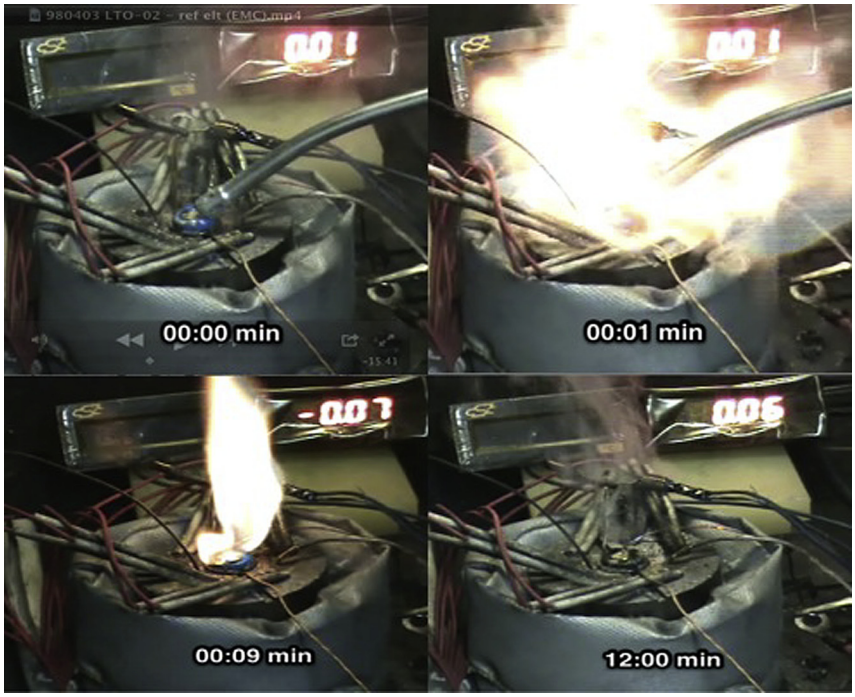

Fig. 15. Flammability test: 18650 cell ($Li_4Ti_5O_{12}$/$LiMn_2O_4$:$Li(Ni_{1/3}Co_{1/3}Mn_{1/3})O_2$) with reference electrolyte E1.

from the pressure vent (Fig. 16), which continued to burn for 1 min. Another sample containing E2 electrolyte tested after high-temperature cycling caused an even smaller fire, which lasted only 17 s after the pressure vent was opened (Fig. 17). This experiment shows that the amount of by-products of TBBA decomposition responsible for its fire extinguishing mechanism is controlled by preconditioning of the battery cell, i.e., fresh, after cycling or after high temperature cycling states.

As an example of the low efficiency of commonly studied flame-retardants (such as trimethyl phosphate (TMP)) we performed a test on an identical cell filled with an electrolyte (1 M LiPF6, EC:EMC, 1:2 vol.) consisting of 5 wt.% of TMP. The sample generated

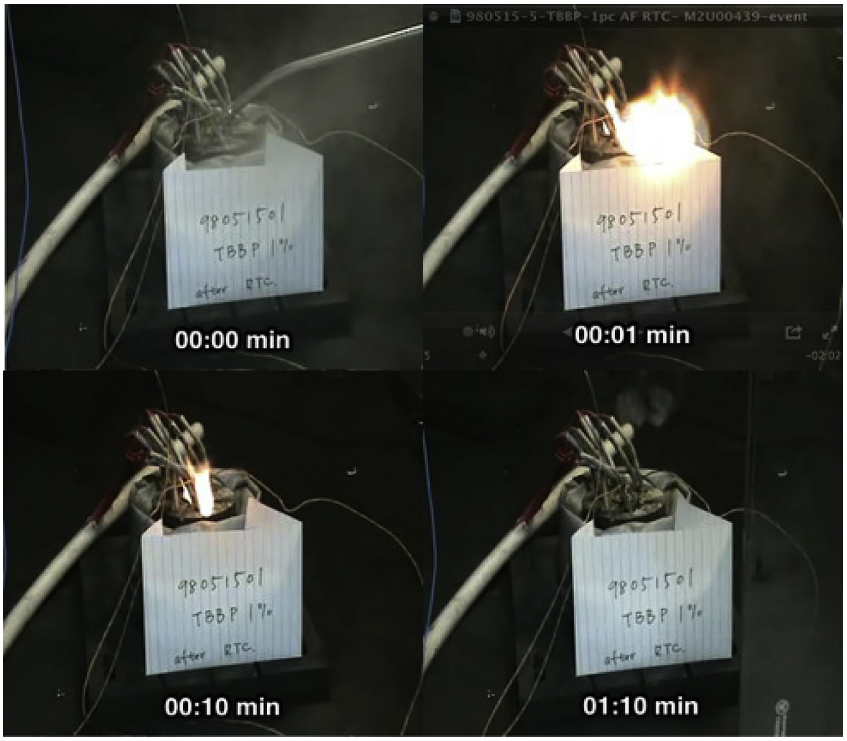

Fig. 16. Flammability test: 18650 cell ($Li_4Ti_5O_{12}$/$LiMn_2O_4$:$Li(Ni_{1/3}Co_{1/3}Mn_{1/3})O_2$) with electrolyte E2 after room temperature cycle test.

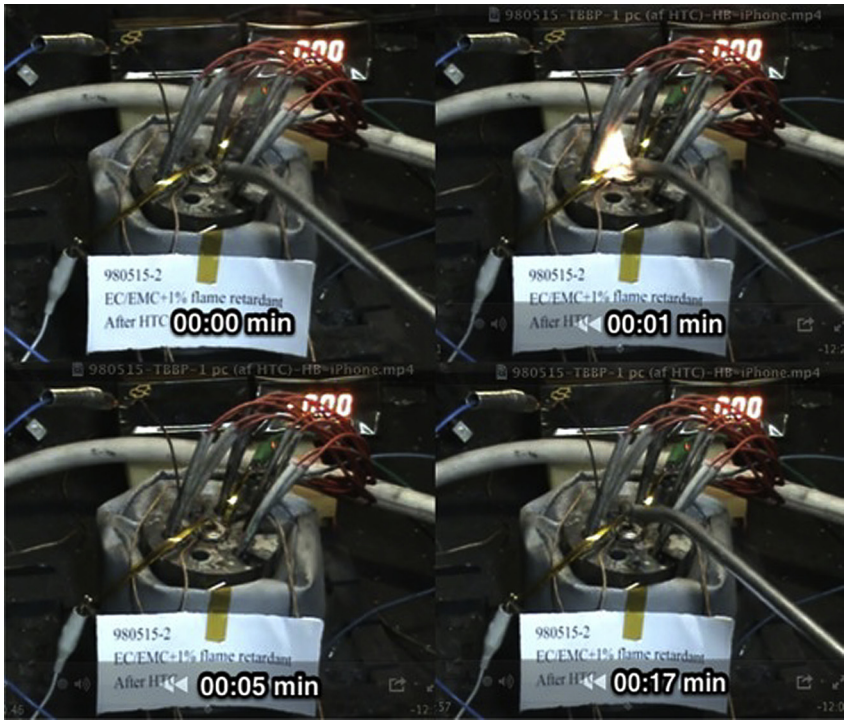

Fig. 17. Flammability test: 18650 cell ($Li_4Ti_5O_{12}/LiMn_2O_4$:$Li(Ni_{1/3}Co_{1/3}Mn_{1/3})O_2$) with electrolyte E2 after high temperature cycle test.

a medium-size fire just as the reference cell had done (Fig. 18) which continued to burn for over 2 min. Comparable amounts of TMP and TBBA were used in the tests.

In order to understand TBBA's fire extinguishing effect in these study, we had to model battery behavior in abnormal conditions. In the case of external heat or mechanical damage (i.e. external short or crush) pressure inside the cell is increased (electrolyte evaporation and decomposition causing the cell to vent). The vented gas is highly combustible as it consists of low boiling point solvents, electrolyte decomposition products [22] such as methane, ethane,

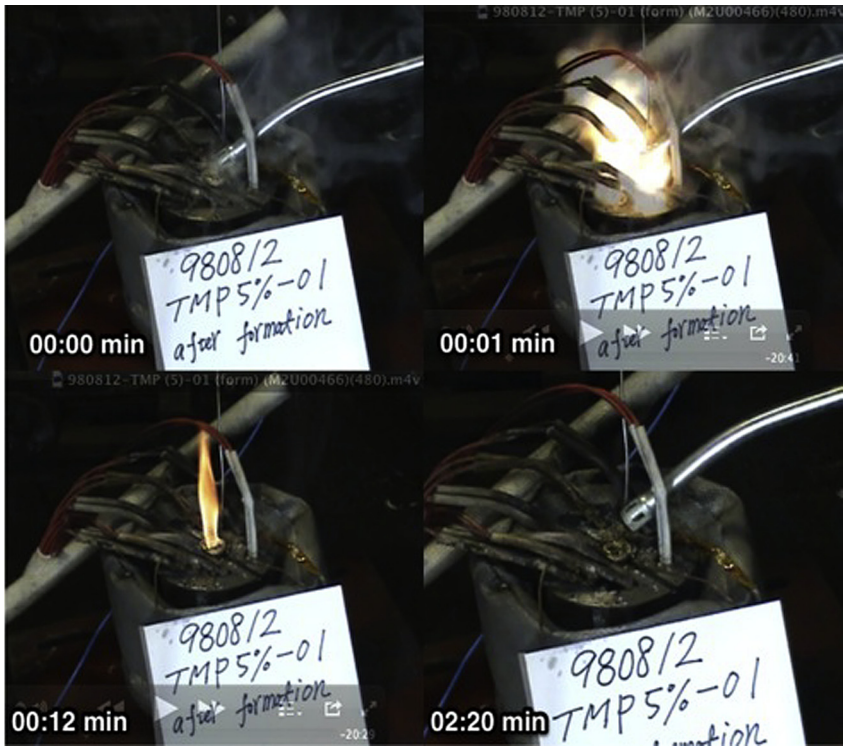

Fig. 18. Flammability test: 18650 cell ($Li_4Ti_5O_{12}/LiMn_2O_4$:$Li(Ni_{1/3}Co_{1/3}Mn_{1/3})O_2$) with 1 M $LiPF_6$, EC:EMC (1:2 vol.) electrolyte and TMP 5 wt.%.

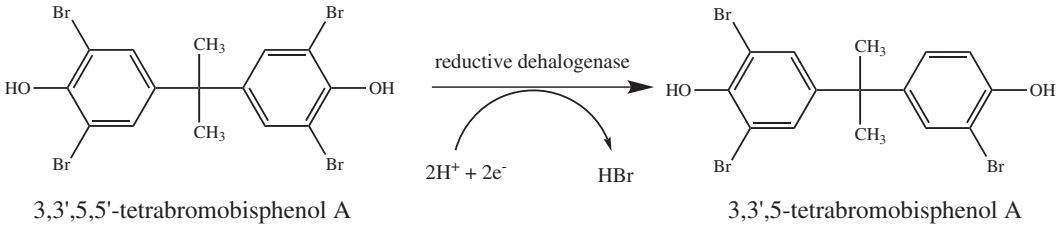

Fig. 19. First stage of the reductive reaction of TBBA/BPA.

oxygen and some others, and is finally, mixed with atmospheric oxygen. At this point, the gas-phase mechanisms of flame-retardants come into effect. In this mechanism, the flame-retarding agent has to be volatile, i.e., mixed and decomposed into gaseous products released from cell body into the atmosphere, and provides the active fraction of molecules in the gaseous phase (Fig. 19).

The decomposition of TBBA has been well studied as it is used as a flame-retardant additive in many materials. Thermal decomposition of TBBA has been studied by Marsanich et al. [23] and Barontini et al. [24]. They show that thermal degradation of TBBA only starts at above 185 °C and becomes relevant just above 230 °C. Even at 210 °C the main gaseous product of TBBA degradation is HBr (≈80 mol %), the second product being tribromobisphenol A (8.6 mol %) (TBA). Thus we can assume that the main mechanism of decomposition of TBBA and TBBA by-products at the heating/burning stage is electrochemical reductive dehalogenation with the main products of the reaction being HBr, Br_2 and TBA, where Br—H is a gas dissolved in the electrolyte solution.

Finally, during an event, the electrolyte solution and its vapors consist mainly of a mixture of H—Br and Br—Br, which, on heating, releases HBr and Br• radicals. These radicals will interfere with the flame chemistry by the following general reactions:

$$RBr \rightarrow R^{\bullet} + Br^{\bullet} \quad (1)$$

$$Br^{\bullet} + R \cdot CH_3 \rightarrow RCH_2^{\bullet} + HBr \quad (2)$$

$$HBr + OH^{\bullet} \rightarrow H_2O + Br^{\bullet} \quad (3)$$

$$H^{\bullet} + HBr \rightarrow H_2 + Br^{\bullet} \quad (4)$$

where R•, $CH_2^{\bullet}$, H• and OH• radicals are parts of the flame oxidative chain reaction that consumes fuel (RCH_3) and oxygen [25]. As a result, vented electrolytes containing TBBA will demonstrate self-extinguishing properties in abnormal conditions.

4. Conclusions

In this study we have tested tetrabromobisphenol A (TBBA) as a flame-retardant additive in a common non-aqueous Li-ion battery electrolyte. We propose that TBBA in Li-ion batteries can serve as flame-retardant by means of the gas-phase mechanism. The influence of the TBBA additive amount (from 0 to 3 wt.%) in the electrolyte on over-all battery properties at different rates and temperatures was evaluated. CV tests on the negative (MCMB) and positive (C—$LiFe_{1-y}Mn_yPO4$) electrodes (vs. Li/Li+) show that TBBA does not undergo electrochemical decomposition on the negative electrode but may affect quality of SEI_{anode} formation by making it more dense or resistant and slowing down Li intercalation at initial cycles. On the positive electrode, competing redox processes are observed between the cathode and TBBA during the first few cycles. Very small amount of by-products of such reactions deposit and remain at the electrode surface as shown by XPS study. We propose that during initial cycles, TBBA undergoes redox decomposition by oxidation reactions at the cathode surface (at catalytic canters, e.g. MnO_2) to form phenoxy radicals that act as redox shuttle molecules. However, due to their instability, such radicals exist only a short time. This consumes a significant amount of charge (current leakage) during fresh cell activation (first few cycles), but does not notably influence the real capacity of the Li-ion battery, i.e., TBBA does not consume Li. The cycling efficiency of 18650 cells containing TBBA is close to 100%. We also demonstrated that the current rate during the initial charge/discharge process controls the rate of TBBA decomposition; the higher the current rate, the lower the amount of TBBA decomposition. Furthermore, according to our more recent studies, using Mn free cathodes or an artificial coating on the cathode surface (i.e. C—$LiFePO_4$, or STOBA) can eliminate TBBA redox decomposition during initial cycles. Finally, burst and flammability tests performed on 18650 cells confirmed TBBA's flame-retardant (self-extinguishing) ability at much lower concentrations (as low as 1 wt.%) than conventional flame-retardant additives.

References

[1] D. Belov, M.-H. Yang, Solid State Ionics 179 (2008) 1816–1821.
[2] S. Tobishima, Y. Ogino, Y. Watanabe, J. Appl. Electrochem. 33 (2003) 143–150.
[3] C. Korepp, W. Kern, E.A. Lanzer, P.R. Raimann, J.O. Besenhard, M. Yang, K.-C. Möller, D.-T. Shieh, M. Winter, J. Power Sources 174 (2004) 637–642.
[4] D. Belov, M.-H. Yang, ECS Trans. 6 (2007) 29–44.
[5] B. Dixon, R. Morris, S. Dallek, J. Power Sources 138 (2004) 274–276.
[6] T. Tsujikawa, K. Yabuta, T. Matsushita, T. Matsushima, K. Hayashi, M. Arakawa, J. Power Sources 189 (2009) 429–434.
[7] J. Feng, X. Ai, Y. Cao, H. Yang, J. Power Sources 177 (2008) 194–198.
[8] H. Ota, A. Kominato, W.-J. Chun, E. Yasukawa, S. Kasuya, J. Power Sources 119-121 (2003) 393–398.
[9] K. Xu, M.S. Ding, S. Zhang, J.L. Allen, T.R. Jow, J. Electrochem. Soc. 149 (2002) A622–A626.
[10] M. Galinski, A. Lewandowski, I. Stepniak, Electrochim. Acta 51 (2006) 5567–5580.
[11] H.-J. Liaw, S.-K. Huang, H.-Y. Chen, S.-N. Liu, Proc. Eng. 45 (2012) 502–506.
[12] A. Guerfi, M. Dontigny, P. Charest, M. Petitclerc, M. Lagacé, A. Vijh, K. Zaghib, J. Power Sources 195 (2010) 845–852.
[13] R.S. Kühnel, N. Böckenfeld, S. Passerini, M. Winter, A. Balducci, Electrochim. Acta 56 (2011) 4092–4099.
[14] D. Doughty, E. Roth, C. Crafts, G. Nagasubramanian, G. Henriksen, K. Amine, J. Power Sources 146 (2005) 116–120.
[15] J.H. Scofield, J. Electron Spectrosc. Relat. Phenom. 8 (1976) 129–137.
[16] S. Ahmad, Ionics 15 (2009) 309–321.
[17] S. Izquierdo-Gonzales, W. Li, B. Lucht, J. Power Sources 135 (2004) 291–296.
[18] K. Xu, S. Zhang, J.L. Allen, T.R. Jow, J. Electrochem. Soc. 150 (2003) A170.
[19] K. Lin, W. Liu, J. Gan, Environ. Sci. Technol. 43 (2009) 4480–4486.
[20] Z. Chen, Q. Wang, K. Amine, J. Electrochem. Soc. 153 (2006) A2215.
[21] C. Buhrmester, J. Chen, L. Moshurchak, J. Jiang, R.L. Wang, J.R. Dahn, J. Electrochem. Soc. 152 (2005) A2390.
[22] K. Kumai, H. Miyashiro, Y. Kobayashi, K. Takei, R. Ishikawa, J. Power Sources 81–82 (1999) 715–719.
[23] K. Marsanich, S. Zanelli, F. Barontini, V. Cozzani, Thermochim. Acta 421 (2004) 95–103.
[24] F. Barontini, K. Marsanich, L. Petarca, V. Cozzani, Ind. Eng. Chem. Res. 43 (2004) 1952–1961.
[25] L.C. Speitel, Toxicology 116 (1996) 167–177.